

INTERNATIONAL SOCIETY FOR SOIL MECHANICS AND GEOTECHNICAL ENGINEERING



This paper was downloaded from the Online Library of the International Society for Soil Mechanics and Geotechnical Engineering (ISSMGE). The library is available here:

<https://www.issmge.org/publications/online-library>

This is an open-access database that archives thousands of papers published under the Auspices of the ISSMGE and maintained by the Innovation and Development Committee of ISSMGE.

The paper was published in the proceedings of the 20th International Conference on Soil Mechanics and Geotechnical Engineering and was edited by Mizanur Rahman and Mark Jaksa. The conference was held from May 1st to May 5th 2022 in Sydney, Australia.

Evaluating shear strain accumulation of sands exhibiting cyclic mobility behavior

Évaluation de l'accumulation de déformation de cisaillement des sables présentant un comportement de mobilité cyclique

Francisco Humire, Katerina Ziotopoulou & Jason T. DeJong

Department of Civil and Environmental Engineering, University of California, Davis, USA, fahumire@ucdavis.edu

ABSTRACT: A series of cyclic stress-controlled constant-volume direct simple shear (CV-DSS) tests were performed to examine the effect of grain properties and gradation on the accumulation of shear strains of soils exhibiting cyclic mobility behavior. A framework to compare patterns of shear strain accumulation per loading cycle was built based on cyclic CV-DSS tests performed on a benchmark material at different relative densities. Strain accumulation patterns of the benchmark material were compared to those obtained for other eight coarse-grained soils with varying grain shapes, grain sizes and gradations. Results showed that an increase on grain angularity and grain size leads to a reduction of the shear strain accumulation per loading cycle. On the other hand, an increase on the coefficient of uniformity (C_u) can lead to an arrest on the shear strain accumulation after exceeding a certain strain threshold, as exhibited by the two well-graded soils presented in this work.

RÉSUMÉ : Une série d'essais de cisaillement simple, direct, à volume constant contrôlé par contrainte cyclique (CV-DSS) a été réalisée pour examiner l'effet des propriétés et de la gradation des grains sur l'accumulation de déformations de cisaillement des sols présentant un comportement de mobilité cyclique. Un cadre pour comparer les modèles d'accumulation de contrainte de cisaillement par cycle de chargement a été construit sur la base d'essais CV-DSS cycliques, effectués sur un matériel de référence à différentes densités relatives. Les modèles d'accumulation de déformation du matériel de référence ont été comparés à ceux obtenus pour huit autres sols à grains grossiers avec des formes de grains, des tailles de grains et des gradations variables. Les résultats ont montré qu'une augmentation de l'angularité et de la taille des grains conduit à une réduction de l'accumulation de contrainte de cisaillement par cycle de chargement. D'autre part, une augmentation de la gradation peut conduire à un arrêt de l'accumulation de déformation de cisaillement, après avoir dépassé un certain seuil de déformation, comme le montrent les deux sols bien gradués présentés dans ce travail.

KEYWORDS: shear strain accumulation, gradation, grain properties, liquefaction, cyclic mobility.

1 INTRODUCTION

The assessment of liquefaction effects requires the ability to estimate ground deformations under a range of in-situ conditions. Among other liquefaction-related phenomena, sands exhibiting cyclic mobility behavior can result in significant lateral deformations as a result of the progressive accumulation of shear strains after liquefaction is triggered. Evidence from laboratory tests on poorly-graded sands shows that the magnitude of cyclic mobility-induced deformations depends on the relative density, shear stress amplitude, and the type of sand tested (Tasiopoulou et al. 2020). Although it is known that the soil behavior is affected by properties such as grain shape (e.g., Cho et al. 2006), grain size (e.g., Hubler et al. 2017), and gradation (e.g., Kokusho et al. 2004), their effect on the post-triggering shear strain accumulation has not been fully understood. Furthermore, recent research at the system level has shown that liquefaction-induced shear deformations on poorly-graded sands are much larger than those exhibited by well-graded materials (Sturm 2019). This knowledge gap regarding the effect of grain properties and particle gradation on the accumulation of shear strains limits current capabilities, from empirical and semi-empirical relationships to constitutive models, to estimate cyclic mobility-induced deformations.

Improved understanding on the cyclic behavior of soils has occurred using element level laboratory tests such as the Constant-Volume Direct Simple Shear (CV-DSS) tests. In comparison to other element level tests (e.g., triaxial, torsional), CV-DSS tests produces a better representation of the in-situ and seismic loading conditions (Finn 1985). Furthermore, since the equivalent undrained conditions are imposed by maintaining a constant height while shearing, previous works show that CV-DSS tests on both dry and saturated specimens of clean sands yield comparable results (Finn and Vaid 1977).

Data interpretation from element-level tests requires a framework for quantitatively assessing the behaviors of interest. The accumulation of post-triggering shear strains in laboratory tests (Figure 1) is typically assessed by tracking the evolution of the double amplitude and single amplitude maximum shear strains (γ_{DA} and γ_{SA}) achieved in each loading cycle. The implementation of this approach shows that the cyclic mobility response in stress-controlled element level tests is characterized by the accumulation of limited shear strains in each loading cycle. The shear strain accumulation can also be characterized by decoupling the shear strains in two components (Shamoto et al. 1997): (1) a strain component that develops at near-zero effective stress (γ_0), and (2) a strain component that develops during dilation (γ_d). The implementation of this framework showed that most of the post-triggering shear deformations are related to strains that develop at near-zero effective stress (Zhang and Wang 2012). In addition, the application of this framework on DEM (Discrete Element Method) simulations of laboratory test results identified particle-level mechanisms associated with the development of post-triggering shear deformations, including the correlation between the evolution of void-based fabric descriptors and the progressive increase of γ_0 in each loading cycle (Wang et al. 2016, Wei et al. 2018).

As part of a broader effort to investigate the characterization and cyclic response of well-graded coarse-grained soils, this paper presents an experimental study to evaluate the effect of grain properties and gradation on the process of shear strain accumulation using cyclic CV-DSS tests. This is achieved by: (1) developing a framework to compare patterns of shear strain accumulation, and (2) evaluating the accumulation of shear strains on different materials encompassing a broad range of grain properties and gradations.

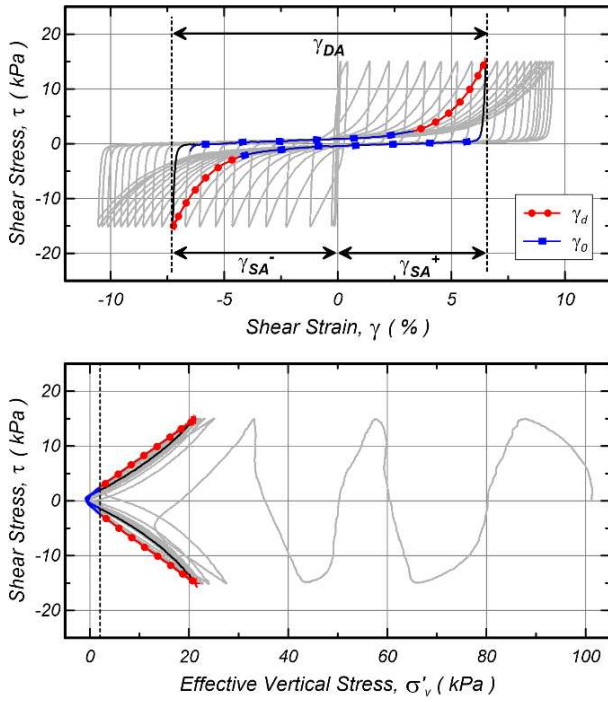


Figure 1. Results of a CV-DSS test performed on a dry specimen of 100A sand with $D_R = 63\%$, including the definitions of double amplitude and single amplitude shear strains (γ_{DA} and γ_{SA}), shear strain at near-zero effective stress (γ_0) and shear strain during dilation (γ_d).

2 EXPERIMENTAL SETUP

2.1 Materials

Coarse-grained soils with different grain properties and gradations were selected for the testing plan presented herein (Table 1). Soils 100A, 100B, 100C and 100D are sub-angular poorly-graded coarse-grained soils with different mean grain sizes (D_{50}) that were sourced from the same natural alluvial deposit (Sturm 2019), and were combined to form soil mixtures with different gradations: 50AB (i.e., 50% 100A, 50% 100B by mass), 33ABC and 25ABCD soils. Given their common geological origin, these soils are expected to isolate the effect of grain size and gradation on the cyclic response of coarse-grained soils.

Table 1. Properties of the soils used in this work: roundness (R) and width-to-length sphericity (S) as defined by Zheng and Hryciw (2015), maximum and minimum void ratio (e_{max} and e_{min}), mean grain size (D_{50}), and coefficient of uniformity (C_u).

Sand	R	S	e_{max}	e_{min}	D_{50} (mm)	C_u
100A	0.39	0.74	0.881	0.579	0.18	1.68
100B	0.40	0.75	0.835	0.524	0.51	1.80
100C	0.42	0.75	0.839	0.557	1.31	1.54
100D	0.45	0.75	0.812	0.540	2.58	1.53
50AB	0.40	0.74	0.753	0.468	0.29	2.82
33ABC	0.40	0.75	0.622	0.397	0.51	4.41
25ABCD	0.41	0.75	0.544	0.303	0.80	7.44
Nevada	0.53	0.76	0.890	0.511	0.14	1.90
Ottawa F-65	0.70	0.77	0.778	0.508	0.20	1.47

In addition to 100A sand, two other fine-grained poorly-graded sands were selected for the testing plan: Nevada (sub-rounded) and Ottawa F-65 (sub-rounded to rounded). This group of fine-grained sands was selected to capture the effect of grain shape on the accumulation of strains. Details regarding the index characterization of Nevada and Ottawa F-65 sands are available in Arulmoli et al. (1992) and Carey et al. (2020), respectively.

2.2 Equipment

The cyclic CV-DSS tests were performed in an Electromechanical Dynamic Cyclic Simple Shear (EMDCSS) device manufactured by GDS Instruments. This device has transducers that measure shear deformations within a range of ± 10 mm and vertical deformations within a range of ± 2.5 mm, both with a 0.1% accuracy. The active height control system implemented in this device allowed the performance of CV-DSS tests with vertical strains below the 0.05% threshold recommended by ASTM (2019).

Most of the tests performed in this work were on specimens of about 18 mm in height and 70 mm in diameter. In order to meet ASTM (2019) requirements regarding grain size and specimen height, tests on the 25ABCD and 100D soils were performed in large-size specimens with a diameter of 150 mm and about 33 mm in height. Specimens were laterally enclosed by a stack of low-friction steel rings and a latex membrane of about 0.35 mm in thickness. Sintered steel porous discs with protruding ridges of 1 mm in height were mounted on the end caps to transmit shear forces to the samples.

2.3 Procedures

Samples were prepared via air pluviation, which consisted of pouring dry sand from a constant height into the specimen container. After applying a vertical stress of 25 kPa, specimens were subjected to a series of pre-conditioning strain-controlled drained cycles with an amplitude of 0.045% shear strain and a frequency of 0.1 Hz to improve the compliance between the top porous ridged disc and specimens. Following the recommendations presented in Humire et al. (2021), a series of cyclic CV-DSS tests were performed on specimens of 100A and 100C sands to determine the appropriate number of pre-conditioning cycles required to ensure a full engagement of the top platen while avoiding significant changes in the soil response. Tests on soils 100A and 100C were performed with cyclic stress ratios (CSR) of 0.10 and 0.08, respectively. Results showed that the application of more than 50 pre-conditioning cycles can lead to a significant increase on the number of loading cycles to trigger liquefaction for medium dense specimens of 100A sand (Figure 2). However, tests with less than 50 pre-conditioning cycles presented problems on the shear stress transfer to specimens of 100C sand due to a lack of coupling between top cap and specimen. Based on these results, 50 pre-conditioning drained cycles were applied for all tests.

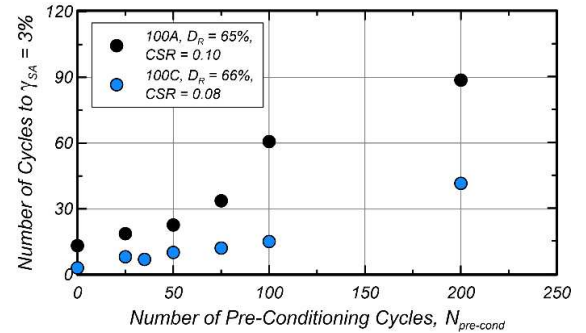


Figure 2. Results of a series of CV-DSS test on soils 100A and 100C to identify the most appropriate number of pre-conditioning drained cycles for this testing plan.

For saturated tests, de-ionized water was flushed from the bottom to the top of the specimens after the application of the pre-conditioning loading cycles. The samples were then consolidated under a vertical stress of 100 kPa and, finally, subjected to a stress-controlled constant-volume cyclic shearing with a loading frequency of 0.05 Hz until a single amplitude shear strain of 10-12% was achieved.

2.4 Relevance of saturation protocols

Preliminary tests performed during earlier stages of this work were affected by partially saturated conditions. Such tests exhibited an unexpected arrest of the accumulation of shear strains per loading cycle at shear strains below 5-6% (Figure 6). It is hypothesized that suction in the soil matrix due to partially saturated conditions artificially increased the resistance to shear deformations on those tests. After the identification of such conditions, the existing saturation protocols were improved by increasing the saturation time (up to 3 hours) and increasing the differential head between the top and bottom of the specimen. Test results obtained after improving the saturation protocols led to the saturated results presented in Figure 3, which exhibited a progressive accumulation of shear strains in each loading cycle instead of the arresting observed for partially saturated conditions.

A series of CV-DSS tests were performed on dry specimens of 100A sand to compare them with the results obtained for saturated specimens. Results showed that CV-DSS tests performed on dry specimens exhibited a response similar to saturated specimens in terms of liquefaction triggering resistance and shear strain accumulation. For example, the dry and saturated tests shown in Figure 4 exhibited negligible differences in their patterns of shear strain accumulation per loading cycle. These results confirm previous observations by Finn and Vaid (1977) and Monkul et al. (2015) on cyclic CV-DSS tests on dry specimens of clean sands yielding to equivalent stress-strain responses than tests on saturated specimens. Given the similarities between the response of dry and saturated specimens, as well as the effect of potential partially saturated conditions on the accumulation of shear strains, it was decided to proceed with CV-DSS tests on dry samples for the rest of the testing plan.

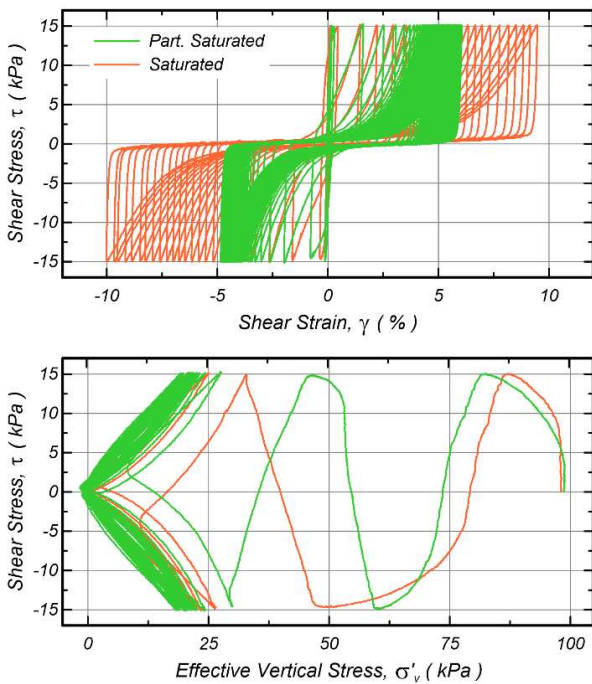


Figure 3. Effect of partially saturated conditions in the CV-DSS results of medium dense specimens of 100A sand ($D_R = 63-68\%$).

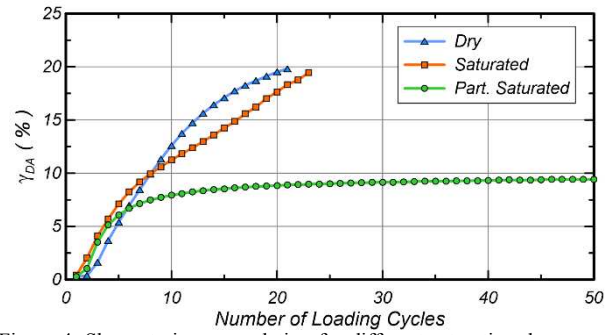


Figure 4. Shear strain accumulation for different saturation degrees on CV-DSS tests performed on medium dense ($D_R = 63-68\%$) specimens of soil 100A with $CSR = 0.15$.

3 DEVELOPMENT OF A FRAMEWORK TO COMPARE PATTERNS OF STRAIN ACCUMULATION

A series of cyclic CV-DSS tests were performed on specimens of 100A sand to develop a framework to compare the patterns of shear strain accumulation of soils with different properties. This sand was selected as the benchmark material given its similar gradation to Nevada and Ottawa F-65 sands, and the common geological origin with the other soils shown in Table 1. Those tests were performed for three different relative densities (D_R) and two cyclic stress ratios (CSR). Figure 5 summarizes the stress-strain loops obtained on tests with a CSR of 0.10, which show a significant decrease of the shear strain increments accumulated in each loading cycle while increasing the relative density. This strong dependency of the shear strain accumulation per loading cycle on the relative density is consistent with the results previously shown in Tasiopoulou et al. (2020).

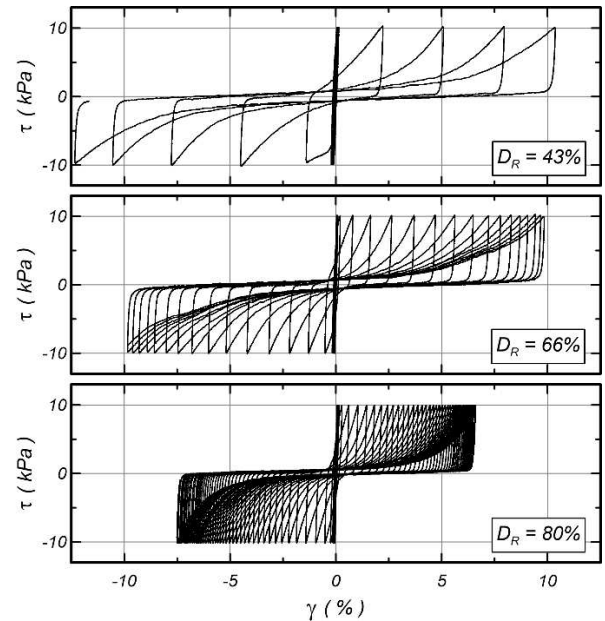


Figure 5. Stress-strain response for CV-DSS tests performed on 100A soil at different relative densities and a cyclic stress ratio (CSR) of 0.10.

In this work, patterns of shear strain accumulation are assessed through the evolution of γ_{DA} (defined in Figure 1) achieved in each loading cycle of the post-triggering regime ($N_{post-trigg}$). A liquefaction triggering criterion of $\gamma_{SA} = 3\%$ was used in this work, and the values of $N_{post-trigg}$ were computed as the difference between the number of loading cycles and the number of cycles to trigger liquefaction. Figure 6 summarizes the patterns of shear strain accumulation observed for 100A for

different D_R and CSR values. The results from tests on the looser samples exhibited an almost linear increasing trend on the accumulation of shear strains per loading cycle for both CSR values. On the other hand, the results on medium dense and dense specimens showed a linear increase in the first loading cycles after triggering, followed by a progressive decrease in the rate of shear strain accumulation per loading cycle at larger strain levels. The progressive decrease of the shear strain increments in each cycle suggests that the accumulation of strains may arrest at a certain threshold and after the application of several loading cycles; however, those deformation levels could not be properly explored due to the limitations of CV-DSS tests to explore large shear strain levels.

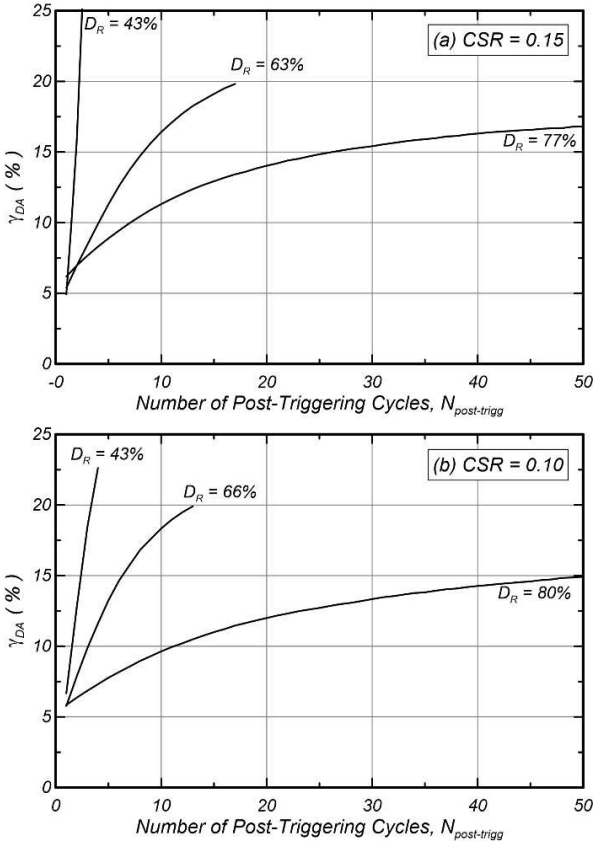


Figure 6. Shear strain accumulation per loading cycle in the post-triggering regime obtained for CV-DSS tests performed on 100A soil at different relative densities and two different cyclic stress ratios (CSR): (a) CSR = 0.15 and (b) CSR = 0.10.

4 SHEAR STRAIN ACCUMULATION ON SANDS WITH DIFFERENT GRAIN PROPERTIES

The framework developed was used to compare patterns of shear strain accumulation for soils with different grain properties (Figure 7). This section presents the results of such comparisons and discussions on the role of grain shape, grain size and gradation on the process of shear strain accumulation.

4.1 Effect of grain shape

In order to explore the effect of grain shape, the patterns of shear strain accumulation of Nevada sand (sub-rounded) and Ottawa F-65 (sub-rounded) were compared to those obtained for 100A sand (sub-angular). The accumulation of shear strains per loading cycle observed for a specimen of Nevada sand with $D_R = 53\%$ was similar to that exhibited by 100A sand at a looser state, while a sample of Ottawa F-65 with $D_R = 67\%$ exhibited a

faster strain accumulation than a test on 100A sand performed at a similar density (Figure 7a). These results show that both Nevada and Ottawa F-65 sands accumulate shear strains faster than 100A sand, which suggest that an increase of grain angularity leads to a reduction of the rate of shear strain accumulation. This effect is attributed to the greater interlocking between particles in angular sands, which results in a greater resistance to shear deformations and an increased dilative behavior.

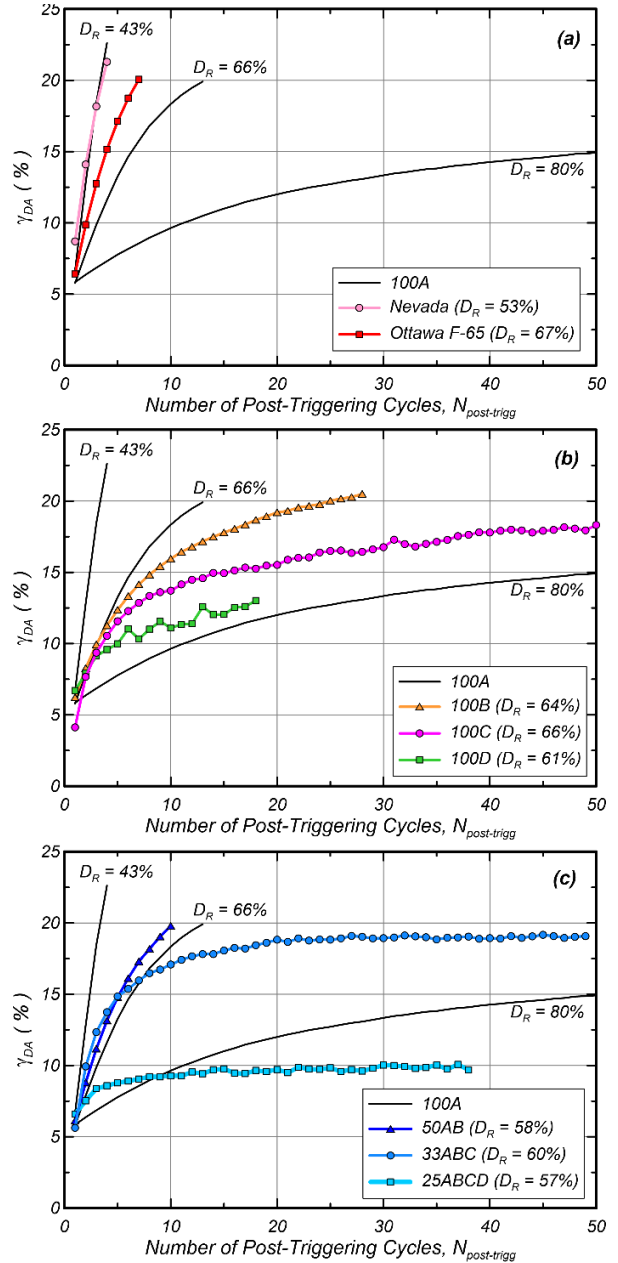


Figure 7. Comparison of the accumulation of shear strains observed in cyclic CV-DSS tests with CSR=0.10 performed on sands with different: (a) grain shape, (b) mean grain size, and (c) gradation.

4.2 Effect of grain size

The effect of mean grain size (D_{50}) on the post-triggering shear strain accumulation was explored by comparing the results obtained for 100A, 100B, 100C and 100D soils for similar relative densities (Figure 7b). The results showed similar rates of shear strain accumulation per loading cycle for the four soils in the first loading cycles after triggering ($\gamma_{DA} = 6-10\%$). After the application of 5 or more post-triggering cycles, the shear strain

increments accumulated in each loading cycle tend to decrease while increasing the grain size. These results suggest that D_{50} mostly affects the process of shear strain accumulation at large strain levels, and finer sands can experience larger post-triggering shear deformations than coarser soils. The smaller rate of shear strain accumulation observed for coarser soils at larger strain levels ($\gamma_{DA} > 10\%$) can be attributed to an enhanced dilation while increasing grain size, which is consistent with the post-liquefaction behaviors observed by Hubler et al. (2017).

4.3 Effect of gradation

The effect of gradation was explored by comparing the CV-DSS tests performed on 100A, 50B, 33ABC, and 25ABCD soils (Figure 7c). The pattern of shear strain accumulation per loading cycle obtained for 50AB sand was similar to that obtained for the medium dense specimen of 100A sand with slight differences attributable to relative density. On the other hand, the test on the 33ABC sand accumulated more shear strains in the first four loading cycles than 100A and 50AB sands; however, a sudden decrease on the rate of shear strain accumulation was observed after those cycles, that led to a full arrest on the accumulation of strains at approximately $\gamma_{DA} = 19\%$ after 20 loading cycles. The test on the 25ABCD soil also exhibited an arrest on the accumulation of shear strains, which occurred at approximately $\gamma_{DA} = 10\%$ after the application of 15 post-triggering loading cycles. This arrest in the accumulation of shear strains was also observed in a second experiment performed on the 33ABC sand but with a different CSR value (Figure 8).

The results obtained for the 33ABC and 25ABCD soils showed that well-graded soils may exhibit a faster shear strain accumulation immediately after triggering, but at the end they can lead to smaller post-triggering shear deformations than poorly-graded fine-grained sands given the arrest on the accumulation of strains. The arrest on the strain accumulation is likely to occur due to a stabilization of changes of the soil fabric in the post-triggering regime and, in particular, of changes in void-based fabric metrics as suggested by previous DEM research (Wang et al. 2016, Wei et al. 2018). It is hypothesized that well-graded materials are limited to smaller shear deformations in comparison to poorly-graded sands due to the smaller voids in the granular assembly, which reduces the particle rearrangement. Finally, the similarities between the shear strain accumulation patterns of 50AB and 100A sands suggest that larger differences in C_u are needed to more reliably and conclusively probe the effect of gradation on the post-triggering response.

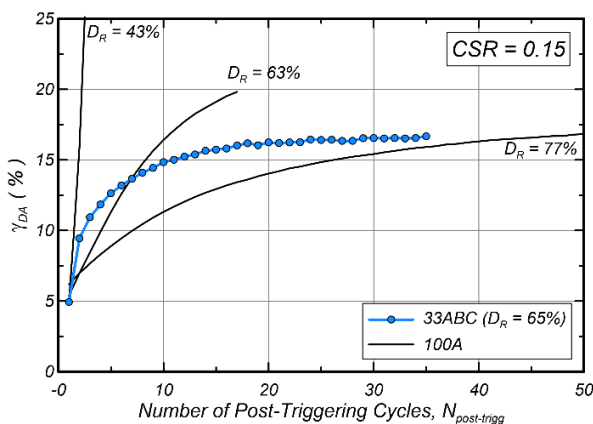


Figure 8. Results of a cyclic CV-DSS tests with $CSR=0.15$ on a medium dense specimen of 33ABC sand.

5 SUMMARY AND CONCLUSIONS

A series of cyclic constant-volume direct simple shear (CV-DSS) tests were performed to investigate differences in shear strain accumulation for sands with different grain properties. A comparison framework was built based on CV-DSS tests performed on a benchmark material (100A sand) at different relative densities. Plots of the double amplitude shear strain as a function of the number of post-triggering loading cycles revealed differences between the benchmark material and other sands. The observations included:

- an increase in grain angularity led to reduction in the rate of shear strain accumulation per loading cycle,
- an increase in grain size led to a reduction in the rate of shear strain accumulation at large strain levels ($\gamma_{DA} = 10\%$), and
- specimens of well-graded coarse-grained soils arrested earlier in strain accumulation after exceeding a certain strain threshold.

The arrest observed on well-graded soils was explained by the smaller amount of voids in the granular assembly and, thus, less room for particle rearrangement during shearing. Therefore, liquefaction-induced deformations on well-graded coarse-grained soils subjected to several cycles after triggering may be smaller than those exhibited by poorly-graded fine-grained sands, consistent with previous findings at the system-level (Sturm, 2019).

Finally, findings from this investigation showed trends regarding the effect of different grain properties on the process of post-triggering shear strain accumulation. For that purpose, the materials selected for the testing plan intended to isolate such grain properties aiming to investigate their effects independently. However, some of the trends may be affected by the influence of other parameters that vary within a same testing group (e.g., differences in D_{50} within the materials used to study the effect of C_u). Further work is necessary to elucidate the combined effect of the different grain properties, as well as the influence of other factors on the process of shear strain accumulation (e.g., fine content, sloping-ground conditions).

6 ACKNOWLEDGEMENTS

The research work presented in this paper was funded by the National Science Foundation (NSF) CMMI Award #1916152. Any opinions, findings, conclusions or recommendations expressed in this paper are those of the authors and do not necessarily reflect the views of NSF. The authors are grateful to Rachel Reardon who was part of the experimental work presented in this paper. The authors are also grateful to Sheikh Sharif Ahmed and Prof. Alejandro Martinez (University of California, Davis) for sharing the results of their image-based grain shape characterization.

7 REFERENCES

- Arulmoli K., Muraleetharan K.K., Hossain M.M. and Fruth L.S. 1992. *VELACS: Verification of liquefaction analysis by centrifuge studies, laboratory testing program*. Soil Data Report, Project No. 90-0562, Earth Technology Corporation, Irvine, CA.
- ASTM International. 2019. *Standard Test Method for Consolidated Undrained Cyclic Direct Simple Shear Test under Constant Volume with Load Control or Displacement Control*. ASTM D8296-19. West Conshohocken, PA: ASTM International, approved November 1, 2019.
- Carey T. J., Stone N. and Kutter B. L. 2020. Grain size analysis and maximum and minimum dry density testing of Ottawa F-65 sand for LEAP-UCD-2017. In Kutter B., Manzari M. and Zeghal M. (eds.) *Model Tests and Numerical Simulations of Liquefaction and Lateral Spreading*, 31-44, Springer, Cham.
- Cho, G.-C., Dodds J. and Santamarina J.C. 2006. Particle shape effects on packing density, stiffness, and strength: natural and crushed

- sands. *Journal of Geotechnical and Geoenvironmental Engineering* 132(5), 591-602.
- Finn W.D.L. 1985. Aspects of constant volume cyclic simple shear. In Khosla V. (ed.) *Advances in the art of testing soils under cyclic conditions*, 74-98, ASCE.
- Finn W.D.L. and Vaid Y.P. 1977. Liquefaction potential from drained constant volume cyclic simple shear tests. *Proc. 6th World Conference on Earthquake Engineering*, New Delhi, India, 2157-2162.
- Hubler J.F., Athanasopoulos-Zekkos A. and Zekkos D. 2017. Monotonic, cyclic, and postcyclic simple shear response of three uniform gravels in constant volume conditions. *Journal of Geotechnical and Geoenvironmental Engineering* 143(9), 04017043.
- Humire F., Lee M., Ziotopoulou K., Gomez M. and DeJong J.T. 2021. Engagement between textured top platens and sand specimens in constant-volume cyclic direct simple shear tests. *Manuscript under review*.
- Humire F., Ziotopoulou K., Singh M.B. and Martinez A. 2019. Framework for tracking the accumulation of shear strains during cyclic mobility. *Proc. 7th International Conference on Earthquake Geotechnical Engineering*, Rome, Italy, 2906-2013.
- Kokusho T., Hara T. and Hiraoka R. 2004. Undrained Shear Strength of Granular Soils with Different Particle Gradations. *Journal of Geotechnical and Geoenvironmental Engineering* 130(6), 621-629.
- Monkul M.M., Gültekin C., Gülver M., Akin Ö. and Eseller-Bayat E. 2015. Estimation of liquefaction potential from dry and saturated sandy soils under drained constant volume cyclic simple shear loading. *Soil Dynamics and Earthquake Engineering* 75, 27-36.
- Shamoto Y., Zhang J.-M. and Goto S. 1997. Mechanism of large post-liquefaction deformation in saturated sand. *Soils and Foundations* 37 (2), 71-80.
- Sturm A.P. 2019. *On the liquefaction potential of gravelly soils: characterization, triggering and performance*. Ph.D. dissertation, Department of Civil and Environmental Engineering, University of California, Davis.
- Tasiopoulou P., Ziotopoulou K., Humire F., Giannakou A., Chacko J. and Travasarou T. 2020. Development and implementation of semiempirical framework for modeling postliquefaction shear deformation accumulation in sands. *Journal of Geotechnical and Geoenvironmental Engineering* 146 (1), 04019120.
- Wang R., Fu P., Zhang J.-M. and Dafalias, Y.F. 2016. DEM study of fabric features governing undrained post-liquefaction shear deformation of sand. *Acta Geotechnica* 11 (6), 1321-1337.
- Wei J., Huang D. and Wang G. 2018. Microscale descriptors for particle-void distribution and jamming transition in pre- and post-liquefaction of granular soils. *Journal of Engineering Mechanics* 144 (8), 4018067.
- Zhang J.-M. and Wang G. 2012. Large post-liquefaction deformation of sand, part I: Physical mechanism, constitutive description and numerical algorithm. *Acta Geotechnica* 7 (2), 69-113.
- Zheng J. and Hryciw R.D. 2015. Traditional soil particle sphericity, roundness and surface roughness by computational geometry. *Geotechnique* 65 (6), 494-506.